BOREAL ENVIRONMENT RESEARCH 19 (suppl. B): 55–70
ISSN 1239-6095 (print) ISSN 1797-2469 (online)

Helsinki 30 September 2014

New instrument for measuring atmospheric concentrations of non-OH oxidants of SO_2

Risto Taipale[1)], Nina Sarnela[1)], Matti Rissanen[1)], Heikki Junninen[1)], Pekka Rantala[1)], Frans Korhonen[1)], Erkki Siivola[1)], Torsten Berndt[2)], Markku Kulmala[1)], Roy L. Mauldin III[1)3)], Tuukka Petäjä[1)] and Mikko Sipilä[1)]*

[1)] *University of Helsinki, Department of Physics, P.O. Box 64, FI-00014 University of Helsinki, Finland (*corresponding author's e-mail: mikko.sipila@helsinki.fi)*
[2)] *Leibniz Institute for Tropospheric Research, Permoserstr. 15, D-04318 Leipzig, Germany*
[3)] *University of Colorado at Boulder, Department of Atmospheric and Oceanic Sciences, P.O. Box 311, Boulder, Colorado 80309, USA*

Received 22 Nov. 2013, final version received 4 Apr. 2014, accepted 9 Apr. 2014

Taipale, R., Sarnela, N., Rissanen, M., Junninen, H., Rantala, P., Korhonen, F., Siivola, E., Berndt, T., Kulmala, M., Mauldin, R. L. III, Petäjä, T. & Sipilä, M. 2014: New instrument for measuring atmospheric concentrations of non-OH oxidants of SO_2. *Boreal Env. Res.* 19 (suppl. B): 55–70.

In addition to the hydroxyl radical (OH), also other oxidants of sulphur dioxide (SO_2) can play a substantial role in the production of atmospheric sulphuric acid (H_2SO_4). Some of these non-OH oxidants are stabilized Criegee intermediates (sCIs) formed in the ozonolysis of alkenes. This paper introduces an FR-CI-APi-TOF instrument which measures the total concentration of all non-OH oxidants (X) reacting with SO_2 at a reasonable rate. The instrument consists of a flow reactor (FR) and a chemical ionisation (CI) atmospheric pressure interface (APi) time of flight (TOF) mass spectrometer. The first field measurements at a boreal forest site indicated that the summer concentration, production rate and apparent lifetime of X were (0.5–8.0) × 10^5 cm^{-3}, (0.3–1.6) × 10^6 cm^{-3} s^{-1} and 0.1–1.8 s, respectively. The estimated concentration and production rate of sCIs formed in the ozonolysis of monoterpenes were substantially lower, possibly indicating the presence of sCIs from other alkenes. Further instrument development is needed to reduce the uncertainties in FR-CI-APi-TOF measurements.

Introduction

Gaseous sulphuric acid is one of the major initiators of atmospheric new particle formation and thus relevant to global climate and air quality (Weber *et al*. 1996, Sipilä *et al*. 2010, Zhang 2010, Kulmala *et al*. 2013). Oxidation of sulphur dioxide (SO_2) by the hydroxyl radical (OH) is considered the main source of sulphuric acid (H_2SO_4). However, recent studies indicate that also non-OH oxidants can play a substantial role in H_2SO_4 production (Mauldin *et al*. 2012, Welz *et al*. 2012, Boy *et al*. 2013, Percival *et al*. 2013).

Some of these non-OH oxidants of SO_2 are stabilized Criegee intermediates (carbonyl oxides) which are formed in the ozonolysis of alkenes (Jiang *et al*. 2010, Berndt *et al*. 2012, Welz *et al*. 2012, Taatjes *et al*. 2013). In addition to SO_2, stabilized Criegee intermediates (sCIs) can react with many other atmospherically relevant compounds, including water vapour, ozone, nitrogen oxides, sulphuric acid, carbonyls and

Editor in charge of this article: Veli-Matti Kerminen

peroxy radicals (Kurtén *et al*. 2007, Taatjes *et al*. 2012, Welz *et al*. 2012, Vereecken *et al*. 2012, Kjaergaard *et al*. 2013). Although tropospheric sCI chemistry is still poorly characterized, there is an emergent consensus that sCIs can have a remarkable effect on the production of atmospheric H_2SO_4 and organic acids, as well as on the NO_x cycle (Bonn and Moortgat 2003, Percival *et al*. 2013, Vereecken 2013, Taatjes *et al*. 2014). However, recent modelling studies suggest that the effect of sCIs on regional sulphate concentrations and the global cloud condensation nuclei budget is only marginal (Li *et al*. 2013, Pierce *et al*. 2013, Sarwar *et al*. 2013). This is partly due to the reactions between sCIs and water vapour and the weak effect of sulphuric acid particle nucleation on cloud condensation nuclei concentrations.

Other non-OH oxidants of SO_2 include peroxy radicals, but their reactions are probably much slower than the reactions between sCIs and SO_2 (Sander and Watson 1981, Kurtén *et al*. 2011). Also some gaseous ions may catalyse SO_2 oxidation and thus contribute to H_2SO_4 production (Bork *et al*. 2013a, 2013b). However, the role of peroxy radicals and ions in regional and global H_2SO_4 production is more uncertain than that of sCIs.

There are several established techniques available for atmospheric OH measurements. These include laser-induced fluorescence, differential optical absorption spectroscopy and chemical ionisation mass spectrometry (Heard and Pilling 2003, Harrison *et al*. 2006, Stone *et al*. 2012). In contrast, measurements of non-OH oxidants of SO_2 are still very limited. Direct measurements of sCIs in laboratory conditions have been based on photoionisation, ultraviolet spectroscopy and infrared absorption (Taatjes *et al*. 2012, 2013, Beames *et al*. 2012, 2013, Welz *et al*. 2012, Su *et al*. 2013). Chemical ionisation mass spectrometry has been utilized for indirect measurements which typically yield the total concentration of all non-OH oxidants which react with SO_2 at a reasonable rate (Berndt *et al*. 2012, Mauldin *et al*. 2012). These techniques have relied on the highly sensitive detection of H_2SO_4 by nitrate-based chemical ionisation at the ambient pressure (Eisele and Tanner 1993, Mauldin *et al*. 1999, Berresheim *et al*. 2000, Petäjä *et al*. 2009, Jokinen *et al*. 2012).

Given the evident atmospheric relevance of non-OH oxidants of SO_2, novel instruments are needed to measure concentrations of these oxidants in different environments. This paper introduces a new technique combining a flow reactor with a chemical ionisation atmospheric pressure interface time of flight mass spectrometer, FR-CI-APi-TOF. The goals here are to demonstrate the suitability of the instrument for ground-based field measurements and to report total concentrations and production rates of the non-OH oxidants observed during the instrument's first field deployment at a boreal coniferous forest site.

Methods

FR-CI-APi-TOF instrument

The instrument (Fig. 1) consists of a flow reactor (FR) and a chemical ionisation atmospheric pressure interface time of flight mass spectrometer (CI-APi-TOF, Jokinen *et al*. 2012). Sample air is pumped through the tubular flow reactor and non-OH oxidants of SO_2 are converted into H_2SO_4 by injecting an excess of SO_2 through injectors at different positions (i.e. reaction times) along the flow reactor axis. Carbon monoxide (CO) is used as an OH scavenger. Upon exiting the flow reactor, H_2SO_4 is ionised in the chemical ionisation region and then detected with the APi-TOF. Thus the instrument measures the total concentration of all non-OH oxidants which react with SO_2 at a reasonable rate but do not react with CO (hereafter termed X), yet it does not identify individual oxidants.

A similar concept has been used in a laboratory setup to study the production of sCIs from the ozonolysis of selected alkenes (Berndt *et al*. 2012). The same indirect detection method has been applied to OH measurements by chemical ionisation mass spectrometry (Eisele and Tanner 1991, Mauldin *et al*. 1998, Petäjä *et al*. 2009), as well as to the first reported field measurements of X (Mauldin *et al*. 2012). The originality of the FR-CI-APi-TOF lies in two aspects. The instrument is a stand-alone unit which is suitable for field measurements and, as explained below, it yields information on both the concentrations and production rates of X.

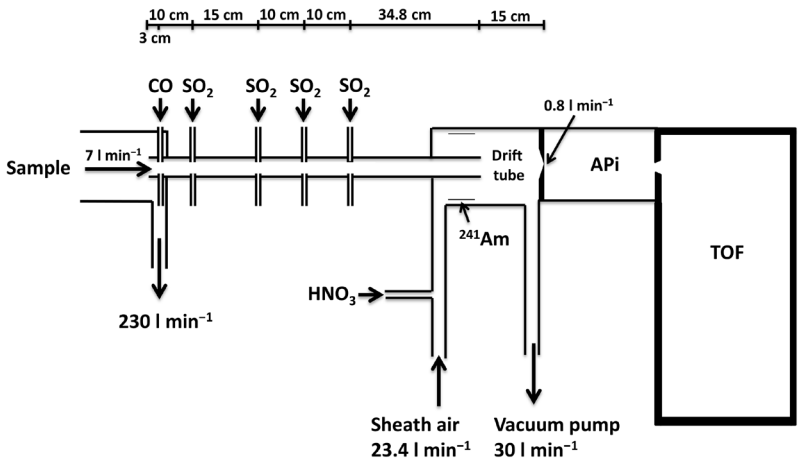

Fig. 1. Configuration of the FR-CI-APi-TOF instrument used in the first field measurements at a boreal coniferous forest site. Sulphur dioxide (SO_2) was injected sequentially through the four injector pairs along the flow reactor (FR) axis to convert all non-OH oxidants of SO_2 (X) into sulphuric acid (H_2SO_4). The H_2SO_4 measurements were based on chemical ionisation (CI) atmospheric pressure interface (APi) time of flight (TOF) mass spectrometry. Nitrate (NO_3^-) reagent ions were produced by feeding nitric acid (HNO_3) containing air into a radioactive ion source (^{241}Am). Carbon monoxide (CO) was used as a hydroxyl radical (OH) scavenger.

In a simplified approach, the measured H_2SO_4 concentration depends on three components:

$$[H_2SO_4] = PR_X t_r + [X]_{amb} + [H_2SO_4]_{amb}, \quad (1)$$

where PR_X is the production rate of X in the flow reactor after the SO_2 injection and t_r is the X–SO_2 reaction time. The terms $[X]_{amb}$ and $[H_2SO_4]_{amb}$ are the ambient (steady state) concentrations of X and H_2SO_4 at the entrance of the flow reactor. Equation 1 is valid for conditions of rapid conversion of X into H_2SO_4 using a large excess of SO_2. Thus it is assumed that the only source of H_2SO_4 in the flow reactor is the X–SO_2 reaction. Wall losses of H_2SO_4 are estimated by calculating diffusion-limited wall loss factors for the different SO_2 injector positions (*see* Eqs. 7–8 below).

The approach described by Eq. 1 is a simplification of the method of Berndt *et al*. (2012) which also includes the effects of sCI losses due to flow reactor walls, thermal decomposition and reactions with water vapour. The simplified approach is applied here since it yielded more physically meaningful results than the more elaborate method. Approximately 4% and 46% of the 228 values of $[X]_{amb}$ were negative when using the two methods, respectively, without constraining their output parameters. This possibly reflects the difference in the measurement conditions. Unlike the field measurements reported here, the measurements of Berndt *et al*. (2012) were conducted in well-defined laboratory conditions using steady state ozone and alkene concentrations. Note that the contribution of ambient H_2SO_4 to Eq. 1 can be substantial in field measurements. It can be minimized using isotopically-labelled $^{34}SO_2$ (instead of normal $^{32}SO_2$) for the conversion of X into $H_2{}^{34}SO_4$.

The reaction time depends on the position of the SO_2 injection, the dimensions of the flow reactor and the sample flow. During a measurement cycle, the reaction time is changed by switching between the different SO_2 injectors (Fig. 2). The last step of the cycle is allocated for determining the ambient H_2SO_4 concentration by feeding SO_2 into an exhaust line instead of the flow reactor. This signal is then subtracted from the signals observed during the other steps. Thus each measurement cycle gives the H_2SO_4 concentration produced in the X–SO_2 reaction as a function of the reaction time. Fitting a linear regression to these data yields the production rate of X (PR_x = slope) and the ambient concentration of X ($[X]_{amb}$ = intercept). An estimate of the apparent lifetime of X is given by

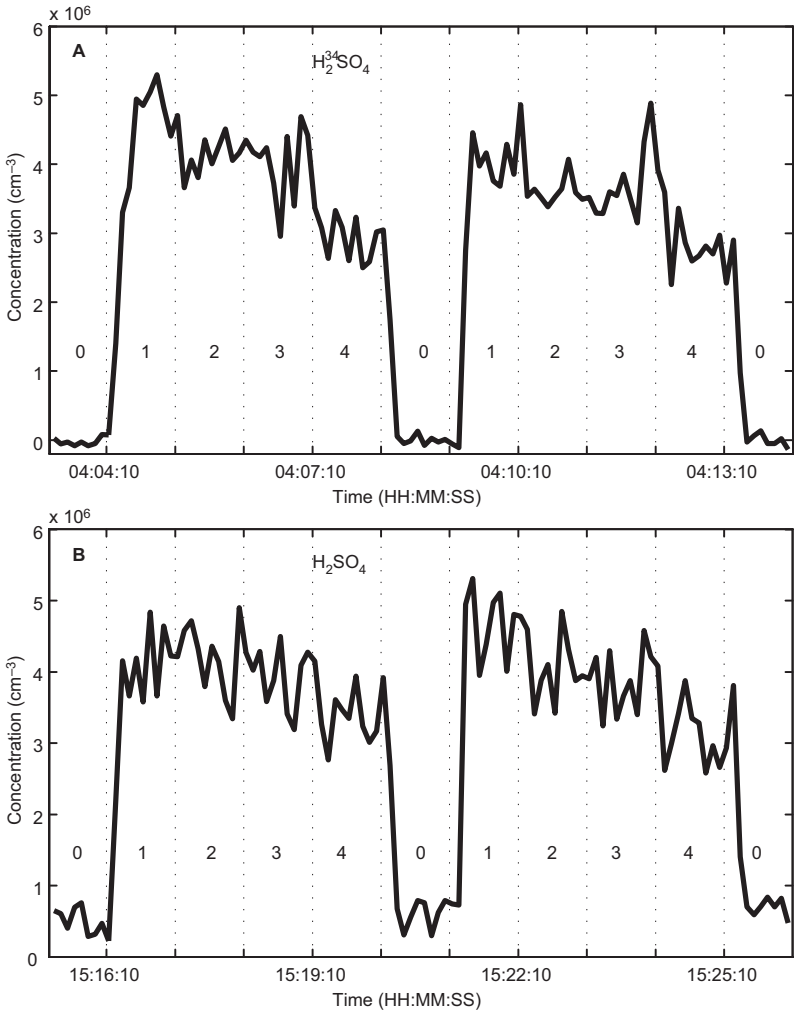

Fig. 2. Examples of FR-CI-APi-TOF measurement cycles observed on (**A**) 10 August 2013 at night, and (**B**) 18 August 2013 in the afternoon. SO_2 was injected sequentially through the four injector pairs (steps 1–4 denoted by the dotted, vertical lines) starting from the one corresponding to the longest reaction time. One step (0) was allocated for the ambient H_2SO_4 measurements when no SO_2 was added to the flow reactor. Isotopically labelled $^{34}SO_2$ was used on 10 August. Therefore, the ambient measurements yielded practically zero concentrations. This figure shows raw measurement data without corrections for H_2SO_4 wall losses in the flow reactor, unlike Figs. 3–5 and 7–8 which include the corrections.

$$\tau = [X]_{amb}/PR_X. \quad (2)$$

The conversion of X into H_2SO_4 can be described by the following simplified reaction sequence (Mauldin *et al*. 1998, Berndt *et al*. 2012):

$$X + SO_2 \rightarrow \ldots \rightarrow SO_3 + X(-O), \quad (3)$$

$$SO_3 + 2H_2O + M \rightarrow H_2SO_4 + H_2O + M. \quad (4)$$

The H_2SO_4 concentration is measured with the CI-APi-TOF (Jokinen *et al*. 2012, Fig. 1). In the CI region of the instrument, nitrate (NO_3^-) reagent ions are produced by flowing air containing nitric acid (HNO_3) over a radioactive source (^{241}Am). This sheath flow and the sample flow are introduced concentrically into an ion drift tube where H_2SO_4 is ionised in proton transfer reactions at ambient pressure:

$$H_2SO_4 + (HNO_3)_{n=0-2}NO_3^- \rightarrow HNO_3HSO_4^- + (HNO_3)_{n=0-2}. \quad (5)$$

Then the ions enter the APi-TOF region where they are guided through the differentially pumped atmospheric pressure interface and finally to the time of flight mass spectrometer for separation according to their mass-to-charge ratios (Junninen *et al*. 2010). A part of the $HNO_3HSO_4^-$ ions fragment into bare HSO_4^- ions in the vacuum of the APi-TOF.

The H_2SO_4 concentration is calculated with the following equation using the measured ion signals:

$$\left[H_2SO_4\right] = C\frac{HSO_4^- + HNO_3HSO_4^-}{NO_3^- + HNO_3NO_3^- + \left(HNO_3\right)_2 NO_3^-} \quad (6)$$

As explained below, the H_2SO_4 calibration coefficient C can be determined directly for the FR-CI-APi-TOF. This enables quantitative X measurements despite the indirect detection method.

To estimate H_2SO_4 wall losses in the flow reactor, wall loss factors are calculated for the different SO_2 injector positions, as well as for the total length of the flow reactor which corresponds to the ambient H_2SO_4 concentration measurement step. The wall loss factor is (Benson *et al*. 2008):

$$\mathrm{WLF} = \frac{\left[H_2SO_4\right]_0}{\left[H_2SO_4\right]_{t_{wl}}} = \frac{\left[H_2SO_4\right]_0}{\left[H_2SO_4\right]_0 e^{-k_{wl}t_{wl}}} = e^{k_{wl}t_{wl}}, \quad (7)$$

where $[H_2SO_4]_0$ is the initial H_2SO_4 concentration and $[H_2SO_4]_{t_{wl}}$ is the H_2SO_4 concentration after the wall loss reaction time t_{wl}. Here it is assumed that the effective wall loss reaction time is half of the corresponding X–SO_2 reaction time. When calculating the wall loss factor for the whole flow reactor, t_{wl} is the total sample residence time in the reactor. For diffusion-limited wall loss of H_2SO_4, the first-order rate coefficient is given by

$$k_{wl} = aD/R^2, \quad (8)$$

where a = 3.65 is an empirical coefficient, D is the diffusion coefficient of H_2SO_4 and R is the flow reactor radius (Hanson and Eisele 2000).

The H_2SO_4 concentrations measured during the SO_2 injection steps are corrected for wall losses using the respective wall loss factors calculated from Eq. 7 and normalised by the wall loss factor for the total length of the flow reactor (*see* the next subsection for details). This normalisation is justified since the wall loss factor for the whole flow reactor is subsumed into the H_2SO_4 calibration coefficient (Eq. 6), i.e. the wall loss correction is unnecessary for the H_2SO_4 concentration observed during the ambient measurement step.

FR-CI-APi-TOF measurements

The first field measurements with the FR-CI-APi-TOF instrument were conducted at the SMEAR II station (Station for Measuring Ecosystem–Atmosphere Relations II; *see* Hari and Kulmala 2005) at Hyytiälä in southern Finland (61°51´N, 24°17´E, 180 m a.s.l.). The measurement periods were 9–11 and 16–18 August 2013. The station is located in the south-boreal vegetation zone and surrounded by a coniferous forest which is dominated by Scots pine (*Pinus sylvestris*) and Norway spruce (*Picea abies*). The undergrowth consists mainly of lingonberry (*Vaccinium vitis-idaea*), bilberry (*Vaccinium myrtillus*) and mosses (*Pleurozium schreberi*, *Dicranum polysetum*). The average tree height near the station was 18–20 m in 2013.

The FR-CI-APi-TOF instrument was installed in an air-conditioned measurement container. An additional stainless steel inlet (length 310 mm, inner diameter 100 mm, flow 230 l min^{-1}) was connected to the flow reactor to minimize artefacts due to the container wall when sampling ambient air (Fig. 1). The sampling height was approximately 1.3 m above the ground.

The stainless steel flow reactor (length 798 mm, inner/outer diameter 16.30/19.05 mm) was connected directly to the ion source and drift tube of the CI-APi-TOF. It contained five pairs of stainless steel injectors (length 19–29 mm of which 5 mm protruded inside the flow reactor, inner/outer diameter 0.25/0.46 mm) installed at 30, 100, 250, 350 and 450 mm downstream from the inlet of the reactor. The sample flow in the flow reactor was 7 l min^{-1} and the total flow in the drift tube was 30.8 l min^{-1} (Fig. 1). The first half of the drift tube (length 150 mm, inner diameter 44 mm) was also assumed to contribute to the reaction times. Based on the injector positions, tube dimensions and flows, the reaction times after the SO_2 injection were 1.47, 1.20, 1.02 and 0.84 s. Similar reaction times with somewhat longer intervals between them were used in the laboratory experiments of Berndt *et al*. (2012).

The first injector pair was used continuously for injecting 300 ml min^{-1} of CO (purity 99.997%) to scavenge OH. The other four injector pairs were used sequentially for injecting

40 ml min^{-1} of N_2 (purity 99.999%) and either 80 ml min^{-1} of $^{34}SO_2$ (0.3% in N_2, 9–11 August) or 100 ml min^{-1} of $^{32}SO_2$ (0.5% in N_2, 16–18 August). These SO_2 flows, corresponding to SO_2 concentrations of (0.8–1.7) × 10^{15} cm^{-3}, were deemed sufficient to convert effectively all X into H_2SO_4 since further increases did not affect the measured H_2SO_4 signal. Similarly, the CO flow, corresponding to 1.0 × 10^{18} cm^{-3}, was tested to be sufficient to scavenge effectively all OH. The OH lifetime under these conditions was around 10 μs, i.e. the OH concentration decreased to 1/*e* of its ambient value during this period. Given the SO_2 concentrations and reaction times, the detected non-OH oxidants had X–SO_2 reaction rates of around 1 × 10^{-15} cm^3 s^{-1} at the minimum. When not used for injecting SO_2 and N_2, a 5 ml min^{-1} flow from the flow reactor to a vacuum pump was applied to each injector pair to ensure that SO_2 entered the flow reactor only from one injector pair at a time.

One FR-CI-APi-TOF measurement cycle consisted of five one-minute steps (Fig. 2). First SO_2 and N_2 were injected through the four different injector pairs for 1 min each, starting from the one corresponding to the longest reaction time. Then SO_2 and N_2 were fed into an exhaust line to determine the ambient H_2SO_4 (or $H_2{}^{34}SO_4$) concentration. The data analysis was based on six-second averages of the CI-APi-TOF data which was originally measured with a pulsing frequency of 12 kHz (Junninen *et al*. 2010). Six successive FR-CI-APi-TOF measurement cycles were merged in the analysis to calculate 30-minute averages of the concentration and production rate of X.

After the measurements, the FR-CI-APi-TOF was calibrated for H_2SO_4 using the same method as Kürten *et al*. (2012). The calibration coefficient $C = 5 \times 10^9$ cm^{-3} is in good agreement with those determined for chemical ionisation quadrupole mass spectrometers (Mauldin *et al*. 1999, Kürten *et al*. 2012). The CI-APi-TOF detection limit for H_2SO_4 is estimated at 3.6 × 10^4 cm^{-3} for a 15-minute averaging period and a similar sampling tube (length 600 mm, outer diameter 19.05 mm) as the flow reactor used here (Jokinen *et al*. 2012).

The H_2SO_4 wall loss factors were calculated using a diffusion coefficient (*D*) of 0.076 cm^2 s^{-1} determined for a relative humidity of 70% (Hanson and Eisele 2000). Thus the wall loss rate coefficient (k_{wl}) was 0.42 s^{-1}. Given the total sample residence time of 1.65 s, the wall loss factor for the total length of the flow reactor was 1.99. The wall loss factors for the SO_2 injector positions were 1.36, 1.29, 1.24 and 1.19, corresponding to normalised values of 0.68, 0.65, 0.62 and 0.60, respectively.

Ancillary measurements

The total monoterpene (MT, $C_{10}H_{16}$) concentration was measured using a proton transfer reaction mass spectrometer (PTR-MS, Taipale *et al*. 2008). Only every third hour was allocated for the ambient concentration measurements since the PTR-MS was used also in volatile organic compound emission measurements with plant enclosures. Linear interpolation was applied to the hourly averages to estimate the monoterpene concentration at 30 min intervals. Other ancillary data were acquired from a set of SMEAR II routine measurements (Junninen *et al*. 2009). These include the SO_2, ozone (O_3) and water vapour (H_2O) concentration as well as the relative humidity (RH), air temperature and global radiation. All ancillary measurements were conducted about 100 m from the FR-CI-APi-TOF container. The measurement height for the gases, relative humidity and temperature (16.8 m) was inside the forest canopy near the tree crowns, while the measurement height for the global radiation (18 m) was right above the canopy. There was a break in the ancillary gas measurements during the first FR-CI-APi-TOF measurement period (9–11 August 2013).

Estimation of sCI concentrations and production rates

The measured concentrations and production rates of X were compared with estimated concentrations and production rates of sCIs produced in the ozonolysis of monoterpenes. The estimation was based on the measured ozone and total monoterpene concentrations. The following reaction pathways were considered:

$$O_3 + MT \rightarrow Y_{sCI}sCI + \ldots, \quad (9)$$

$$sCI + H_2O \rightarrow \text{products}, \quad (10)$$

$$sCI \rightarrow \text{products}. \quad (11)$$

The reactions of sCIs with water vapour (Eq. 10) and the unimolecular decomposition (Eq. 11) were assumed to be the main processes describing the atmospheric fate of sCIs. The resulting sCI production rate PR_{sCI} and the steady state sCI concentration $[sCI]_{ss}$ were calculated from:

$$PR_{sCI} = Y_{sCI}k_{O_3+MT}[O_3][MT], \quad (12)$$

$$[sCI]_{ss} = PR_{sCI}/k_{loss}. \quad (13)$$

The value of the sCI yield $Y_{sCI} = 0.22$ was derived from α-pinene ozonolysis experiments at the Leibniz Institute of Tropospheric Research (T. Berndt, pers. comm.). The ozone–α-pinene reaction rate coefficient was $k_{O_3+MT} = 1.1 \times 10^{-16}$ cm^3 s^{-1} (Witter *et al*. 2002) and a value determined for 1-methyl-cyclohexene at 20 °C, $[H_2O] = 2.9 \times 10^{17}$ cm^{-3} and RH = 50% was used for the sCI loss rate $k_{loss} = k_{10}[H_2O] + k_{11} = 2.4$ s^{-1} (Berndt *et al*. 2012).

Results and discussion

Performance of the FR-CI-APi-TOF instrument

In the first field measurements with the FR-CI-APi-TOF, the measurement cycle consisted of five one-minute steps. As demonstrated by the example cycles in Fig. 2, there was typically a clear decreasing trend in the H_2SO_4 concentration when the reaction time was shortened by switching the position of the SO_2 injection (steps 1–4). When no SO_2 was injected into the flow reactor (step 0), the H_2SO_4 concentration was much lower than during the injection steps and remained essentially at the same level between the two successive measurement cycles. Also the decrease and increase in the H_2SO_4 concentration were rapid when entering and leaving this measurement step.

These findings indicate a fast response time of the FR-CI-APi-TOF and minor memory effects which could be caused by injected SO_2 drifting in the flow reactor. Given the minor role of memory effects, these results suggest that the H_2SO_4 signal measured during step 0 serves as an upper limit estimate of the ambient H_2SO_4 concentration even if normal $^{32}SO_2$ is used (Fig. 2B) and no independent H_2SO_4 measurements are available. On the other hand, ambient H_2SO_4 (and SO_2) do not disturb the FR-CI-APi-TOF measurements substantially since the ambient H_2SO_4 signal is subtracted from the signals measured during the injection steps when determining the X concentration and production rate. Isotopically labelled $^{34}SO_2$ naturally enables more accurate determination of ambient and flow reactor processes and does not disturb the ambient H_2SO_4 measurements, but it is also more expensive and difficult to acquire.

Although the decreasing trend in the H_2SO_4 concentration was often clear (Fig. 2), the noise in the signal typically prevented a meaningful determination of the X concentration and production rate from a single measurement cycle. To better enable a determination, six successive measurement cycles were merged to calculate 30-minute average concentrations and production rates. As illustrated by the 95% confidence intervals in Fig. 3, the 30-minute average H_2SO_4 concentration exhibited a statistically significant increase as a function of the reaction time. The linear least squares fit yielded the average X concentration (intercept) and production rate (slope). Occasionally the fit was reasonably good and, as revealed by the coefficient of determination (r^2), explained around 90% of the changes in the H_2SO_4 concentration. However, the 95% confidence intervals of the X concentration and production rate were often very wide and not always physically meaningful, e.g. (–2.5 to 3.2) $\times 10^6$ cm^{-3} and (–0.7 to 4.2) $\times 10^6$ cm^{-3} s^{-1} in Fig. 3A and (–0.7 to 1.3) $\times 10^6$ cm^{-3} and (0.5 to 2.2) $\times 10^6$ cm^{-3} s^{-1} in Fig. 3B.

To evaluate the performance of the FR-CI-APi-TOF during the field measurements in August 2013, the measurements were categorised into three groups according to the coefficient of determination: high ($r^2 \geq 0.66$), medium ($0.33 \leq r^2 < 0.66$) and low ($r^2 < 0.33$) quality. Here r^2 indicates what proportion of the variation in the 30-minute average H_2SO_4 concentration

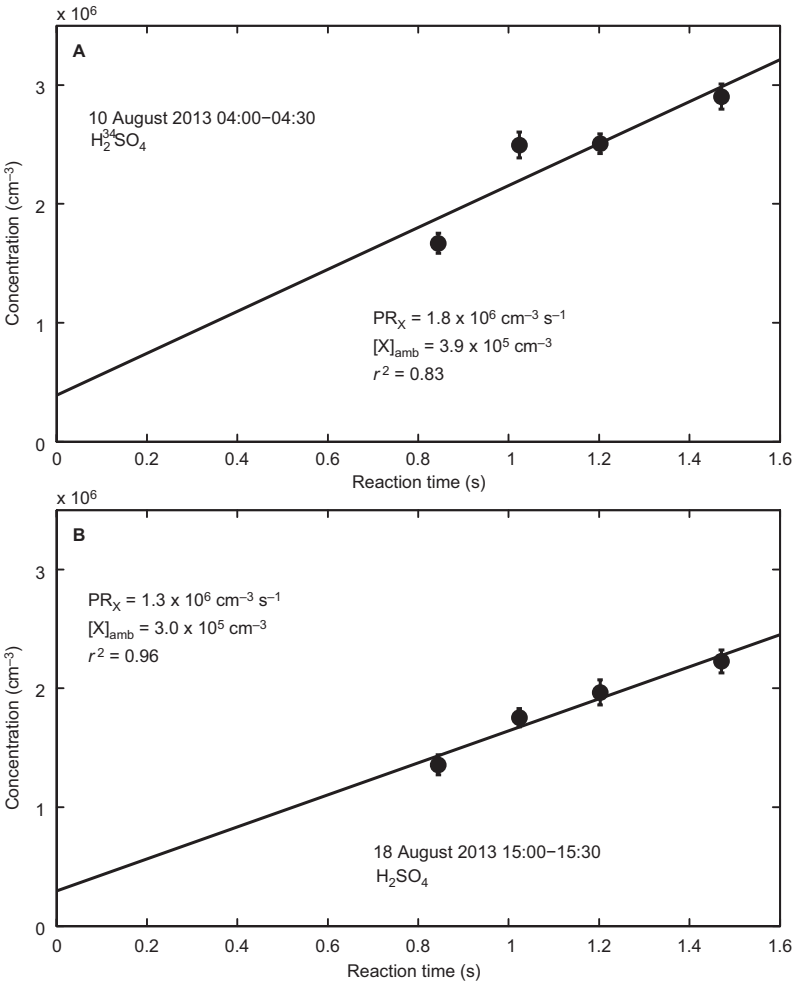

Fig. 3. Determination of the production rate (PR_X) and ambient concentration ($[X]_{amb}$) of all non-OH oxidants of SO_2 (X) from two 30-minute averaging periods. The line shows the linear least squares fit to the average H_2SO_4 concentrations. The error bars represent the 95% confidence intervals and r^2 is the coefficient of determination.

as a function of the reaction time (*see* examples in Fig. 3) is explained by the linear approach to determining the X concentration and production rate (Eq. 1). As seen in Fig. 4, almost all measurements on 9 August were of high quality. Then the quality suddenly decreased and remained at a medium or low level until 12 August. Again, almost all measurements during the second period were of high quality, without a clear temporal pattern in r^2. The only evident alteration to the measurement setup between the first and second periods was the exchange of $^{34}SO_2$ for $^{32}SO_2$. However, $^{34}SO_2$ alone cannot explain the change in the quality given the high quality measurements on 9 August. There were light showers on 10 August, but the decrease started already before then and there were also more intense showers on 17 August. The quality of the measurements correlated with the air temperature (Fig. 5) more clearly during the first period. The correlation coefficients between r^2 and the temperature for the two periods were 0.67 (95% confidence interval: 0.56–0.76) and 0.31 (0.13–0.47), respectively.

In total, 58% of the FR-CI-APi-TOF measurements were of high quality, 27% of medium quality and 15% of low quality. During the second measurement period, the proportion of the high quality measurements was as high as 97%, indicating that the FR-CI-APi-TOF has potential for evolving into a reliable field instrument. Although this quality classification is somewhat subjective with respect to its thresholds, it offers quantitative estimates of the per-

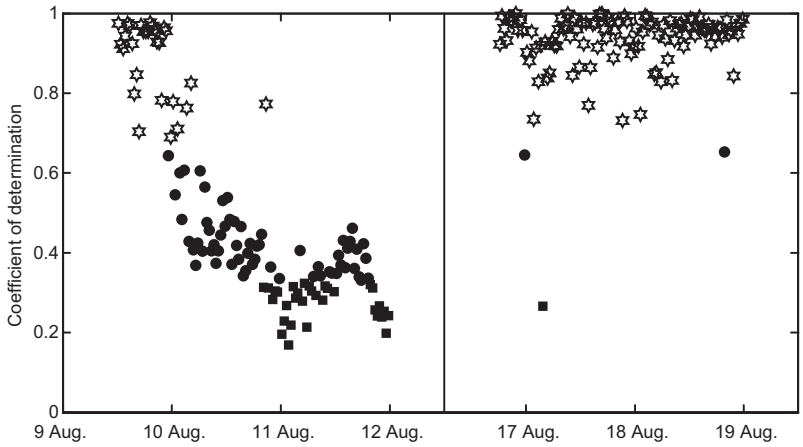

Fig. 4. Coefficients of determination (r^2) for the linear fits to the 30-minute averaging periods in August 2013 (*see* Fig. 3 for details). The stars, dots and squares denote the measurements classified as high ($r^2 \geq 0.66$), medium ($0.33 \leq r^2 < 0.66$) and low ($r^2 < 0.33$) quality, respectively.

formance in terms of the linearity of the instrument, i.e. the validity of Eq. 1 to describe the indirect measurement method of X. Given the wide 95% confidence intervals of the X concentration and production rate, which were typically 100%–400% of the measured values even during the second period, the results presented below should be regarded as uncertain first estimates. Nevertheless, together with the measurements by Mauldin *et al*. (2012) they should provide a baseline for future field measurements of X in boreal environments.

One option to reduce the measurement uncertainties is to add additional injectors to the flow reactor, possibly closer to the ion source, since the main factor contributing to the wide 95% confidence intervals was the linear fit to only four observations. A laboratory experiment with known SO_2, ozone and alkene concentrations would also help to characterise the flow reactor chemistry in more detail, including an estimation of the FR-CI-APi-TOF detection limit for X. When using normal $^{32}SO_2$, the detection limit is probably mainly determined by the ambient H_2SO_4 concentration which has to be subtracted from the H_2SO_4 signals measured during the SO_2 injections. The CI-APi-TOF detection limit for H_2SO_4 (3.6×10^4 cm^{-3}, Jokinen *et al*. 2012) determines the minimum detection limit of the FR-CI-APi-TOF. Given that CO possibly reacts with sCIs at a reasonable rate, operating the FR-CI-APi-TOF with another OH scavenger such as furan might also yield valuable information on the reliability of X measurements.

X concentrations, production rates and lifetimes at a boreal coniferous forest

The X concentration increased monotonously from 0.2×10^6 cm^{-3} to 1.8×10^6 cm^{-3} during the first period (Fig. 5A) when most measurements were of medium or low quality. In contrast, the concentration exhibited more variation during the second period when most measurements were of high quality. The minima of 5×10^4 cm^{-3} were measured on 16 August at midnight and on 18 August at noon, the maxima of 0.8×10^6 cm^{-3} on 17 August in the evening. Apart from the minima during the second period, this X concentration range agrees well with the range of $(0.3–2.0) \times 10^6$ cm^{-3} measured by Mauldin *et al*. (2012) at the same site in late July and early August 2010. Daytime OH concentrations measured by Mauldin *et al*. (2012) were around 1×10^6 cm^{-3}. Petäjä *et al*. (2009) measured similar daytime OH concentrations at the site in March–June 2007.

In the measurements by Mauldin *et al*. (2012), the production of X in the flow reactor of their chemical ionisation mass spectrometer may have contributed to the measured X concentration, thus increasing the reported ambient concentrations. This phenomenon was one major motivation for developing the FR-CI-APi-TOF based on the multiple SO_2 injection positions. Recently, Berresheim *et al*. (2014) introduced a calculation method for estimating the contribution of X production in a similar instrument as the one used by Mauldin *et al*. (2012). They

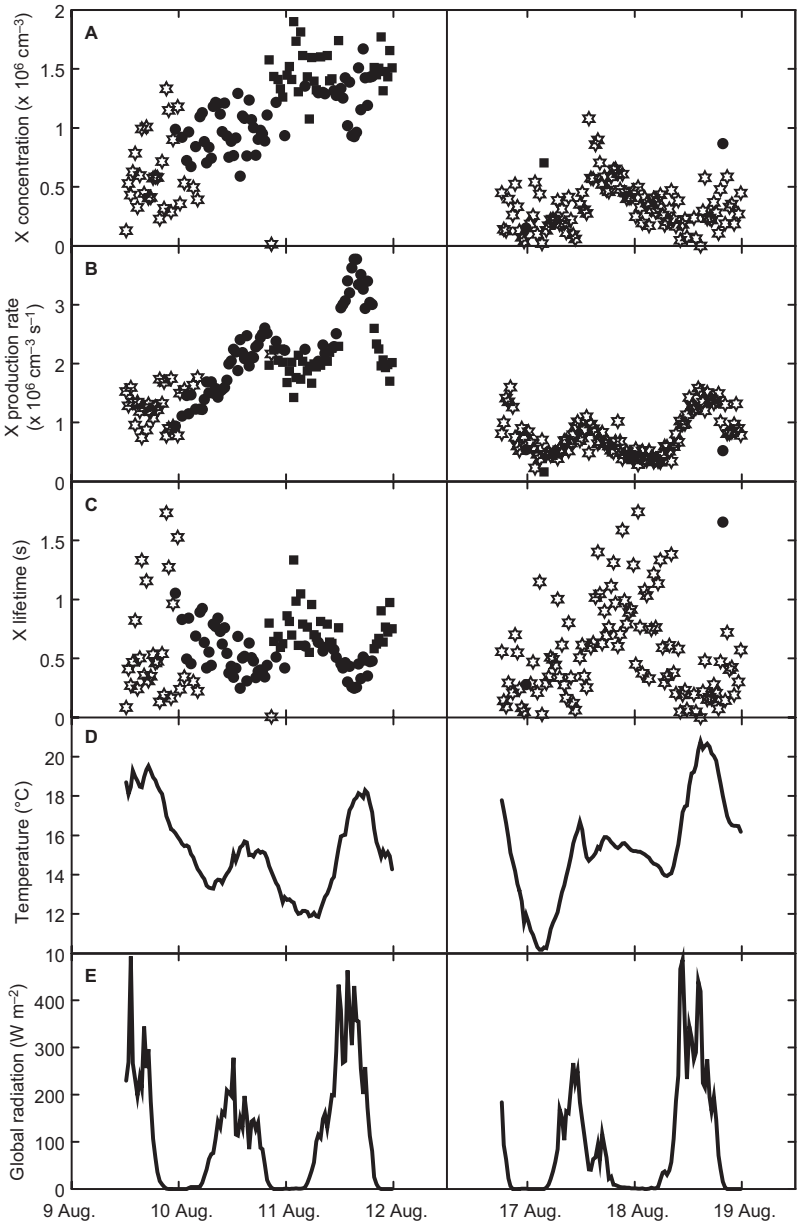

Fig. 5. Concentration, production rate and apparent lifetime of all non-OH oxidants of SO_2 (X), air temperature and global radiation at a boreal forest site in August 2013. The stars, dots and squares denote the measurements classified as high ($r^2 \geq 0.66$), medium ($0.33 \leq r^2 < 0.66$) and low ($r^2 < 0.33$) quality, respectively. Eight concentration values and eleven lifetime values are not shown in **A** and **C**.

measured X concentrations of (0.4–1.6) × 10^6 cm^{-3} at a coastal site in Ireland. Estimates of ambient sCI concentrations range from 2 × 10^4 cm^{-3} for low polluted areas to 2 × 10^6 cm^{-3} for polluted areas (Welz *et al*. 2012, Vereecken *et al*. 2012). Thus the highest X concentrations reported here and by Mauldin *et al*. (2012) are similar to the calculated sCI concentrations for polluted areas, although the measurement site can be regarded as a low-polluted area.

The X production rate had a diurnal cycle during both measurement periods (Fig. 5B). The medium and low quality measurements on 10–11 August yielded the highest production rates with the diurnal maxima around (2.5–3.8) × 10^6 cm^{-3} s^{-1} and the diurnal minima around (1.0–2.0) × 10^6 cm^{-3} s^{-1}. On average, the production rate was more than two times lower during the second period. The highest values around (1.0–1.6) × 10^6 cm^{-3} s^{-1} were observed around noon and the

lowest values around (0.3–0.5) × 10^6 cm^{-3} s^{-1} after midnight.

The apparent lifetime of X derived from the measured concentration and production rate (Eq. 2) varied from around 0.1 s to 1.8 s (Fig. 5C). The lifetime range did not differ remarkably between the measurement periods. There was no clear diurnal cycle, except in the medium and low quality measurements on 10–11 August. Interestingly, the lifetime increased when the showers started on 17 August around noon. Berndt *et al*. (2012) measured lifetimes of 0.3–0.5 s at 20 °C and a relative humidity of 50% for sCIs from the ozonolysis of 2,3-dimethyl-2-butene, trans-2-butene and 1-methyl-cyclohexene using an atmospheric pressure flow tube. Thus the shortest X lifetimes observed in this field study are in agreement with the results of Berndt *et al*. (2012) which were determined in laboratory conditions.

The high quality measurements on 9 August yielded similar X concentrations and production rates as the measurements in the second period, while most medium and low quality measurements on 10–11 August gave consistently higher results. This suggests that the linear approach described by Eq. 1 overestimates the X concentration and production rate when the measurement quality is medium or low. However, more measurements are needed to determine whether this is a systematic feature of the linear approach.

To determine correlation coefficients of the X concentration, production rate and apparent lifetime with the ancillary measurements (Figs. 5–6) and the ambient H_2SO_4 concentration measured with the FR-CI-APi-TOF (Fig. 7), only the results corresponding to the high quality X data from the second measurement period were taken into account (Figs. 4–5). The X concentration correlated positively with relative humidity and water vapour and ozone concentrations (Table 1). Its correlation with global radiation and monoterpene, SO_2 and H_2SO_4 concentrations was negative. As discussed below, the negative correlation with the estimated sCI concentration due to the ozonolysis of monoterpenes was weak but still statistically significant ($p < 0.05$). The correlation between the X concentration and the temperature was insignificant.

The X production rate correlated positively with temperature, global radiation, and SO_2 and H_2SO_4 concentrations. It showed a clear negative correlation with relative humidity and no correlations with monoterpene, ozone and water vapour concentrations. The X lifetime did not correlate with temperature. Instead, it correlated

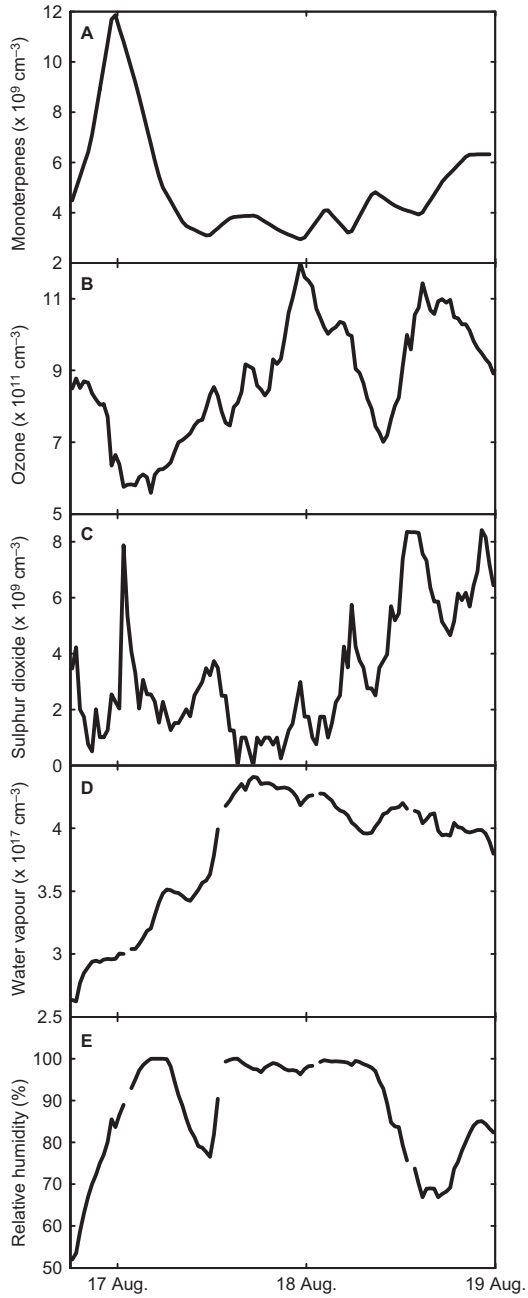

Fig. 6. Ancillary gas concentration and relative humidity measurements during the second FR-CI-APi-TOF measurement period in August 2013.

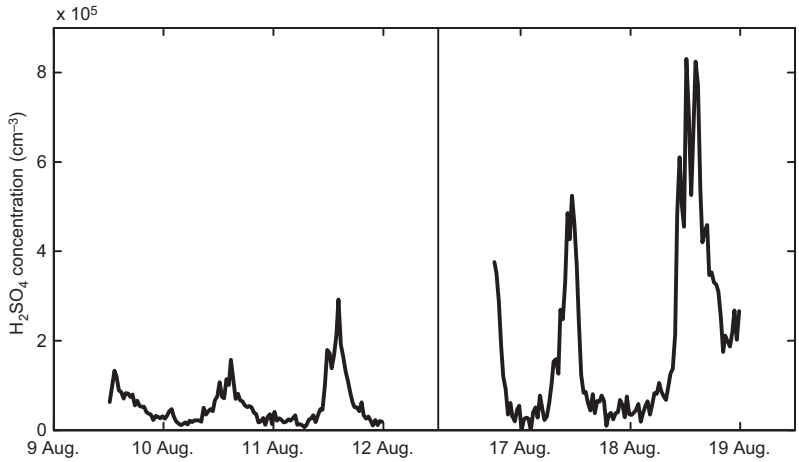

Fig. 7. Ambient H_2SO_4 concentration at a boreal forest site in August 2013. The measurements were conducted with the FR-CI-APi-TOF. Isotopically labelled $^{34}SO_2$ was used in the SO_2 injections between 9 and 11 August, which did not interfere with the ambient H_2SO_4 measurements. Normal $^{32}SO_2$ was used between 16 and 18 August. To minimize its interference, the H_2SO_4 concentration was derived from the ambient signal steps of the FR-CI-APi-TOF measurement cycle (Fig. 2).

positively with relative humidity, and water vapour and ozone concentrations and negatively with global radiation, and monoterpene, SO_2 and H_2SO_4 concentrations. Thus the correlation analysis indicates that the X chemistry at the site might be more complex than oxidation of SO_2 by sCIs from the ozonolysis of monoterpenes (*see* also discussion below).

During the first measurement period, the X concentration was on average around 18 times higher than the H_2SO_4 concentration (Fig. 7). As discussed above, the X concentration was probably overestimated due to the low quality of the FR-CI-APi-TOF measurements. However, the X concentration exceeded the H_2SO_4 concentration also during the second period when most measurements were of high quality, although only by around 80%. This suggests that the oxidation of SO_2 was not the only significant loss mechanism of X in ambient air. The reaction with water vapour was most likely another major sink of X, and also carbonyl compounds such as formalde-

Table 1. Pearson's correlation coefficients of the concentration, production rate and apparent lifetime of all non-OH oxidants of SO_2 (X) with the ancillary variables, the H_2SO_4 concentration and the concentration and production rate of stabilized Criegee intermediates (sCIs) formed from the ozonolysis of monoterpenes. The H_2SO_4 concentration was measured with the FR-CI-APi-TOF. The sCI concentration and production rate were estimated using the measured monoterpene and ozone concentrations. Only the results corresponding to the high quality FR-CI-APi-TOF data (Figs. 4–5) from the second measurement period (16–18 August 2013) were included in the analysis. The numbers in the parentheses are the 95% confidence intervals.

	X concentration	X production rate	X lifetime
Air temperature	0.14 (–0.07 to 0.33)	0.70 (0.58 to 0.79)	–0.16 (–0.35 to 0.04)
Global radiation	–0.26 (–0.44 to –0.06)	0.47 (0.30 to 0.61)	–0.40 (–0.56 to –0.22)
Monoterpenes	–0.35 (–0.51 to –0.15)	0.13 (–0.08 to 0.32)	–0.37 (–0.53 to –0.18)
Ozone	0.26 (0.06 to 0.44)	0.19 (–0.01 to 0.38)	0.24 (0.04 to 0.42)
Sulphur dioxide	–0.35 (–0.52 to –0.16)	0.48 (0.31 to 0.62)	–0.44 (–0.59 to –0.27)
Water vapour	0.48 (0.31 to 0.63)	–0.09 (–0.30 to 0.12)	0.44 (0.25 to 0.59)
Relative humidity	0.26 (0.06 to 0.45)	–0.74 (–0.82 to –0.63)	0.53 (0.36 to 0.66)
Sulphuric acid	–0.32 (–0.49 to –0.13)	0.67 (0.54 to 0.77)	–0.51 (–0.65 to –0.35)
sCI concentration	–0.23 (–0.41 to –0.03)	0.36 (0.16 to 0.52)	–0.32 (–0.49 to –0.13)
sCI production rate	–0.23 (–0.41 to –0.03)	0.36 (0.16 to 0.52)	–0.32 (–0.49 to –0.13)

hyde, acetaldehyde and acetone probably contributed to the loss of X (Vereecken *et al*. 2012). Therefore combined X, OH and H_2SO_4 measurements would probably yield new information on the H_2SO_4 production and the X oxidation capacity towards other compounds than SO_2.

Comparison between the X measurements and the sCI estimations

The sCI concentration and production rate were estimated from the measured monoterpene and ozone concentrations during the second measurement period (Eqs. 12 and 13). The sCI estimations yielded substantially lower values than the X measurements (Fig. 8). The results imply that the contributions of sCIs from the ozonolysis of monoterpenes to the X concentration and the production rate were on average only 23% and 16%, respectively. The contribution to the X concentration was highest when the monoterpene concentration was elevated on 16–17 August (Fig. 6). The contribution of sCIs to the X production rate had distinct nighttime maxima and daytime minima (Fig. 8B).

One reason for the low sCI contribution to the X concentration and production rate is that only monoterpenes were taken into account in the sCI estimations. Another reason is that only α-pinene was considered in the sCI yield and the ozone–monoterpene reaction rate coefficient (Eq. 12). The coniferous forest at the measurement site and boreal forests in general emit also other monoterpenes and various sesquiterpenes ($C_{15}H_{24}$; Hakola *et al*. 2006, Rinne *et al*. 2009), which may have higher sCI yields and reactivities towards ozone, as well as multiple unsaturated bonds capable of producing many sCIs from a single precursor molecule. Given the high reactivity of sesquiterpenes with ozone, they probably play a major role in the sCI production at the site. Isoprene (C_5H_8) is another biogenic compound that is deemed to participate effectively in the sCI chemistry (Taatjes *et al*. 2014). The isoprene concentration was measured at the site but it was mainly below the detection limit of the PTR-MS (Taipale *et al*. 2008). Thus isoprene was not included in the sCI estimations.

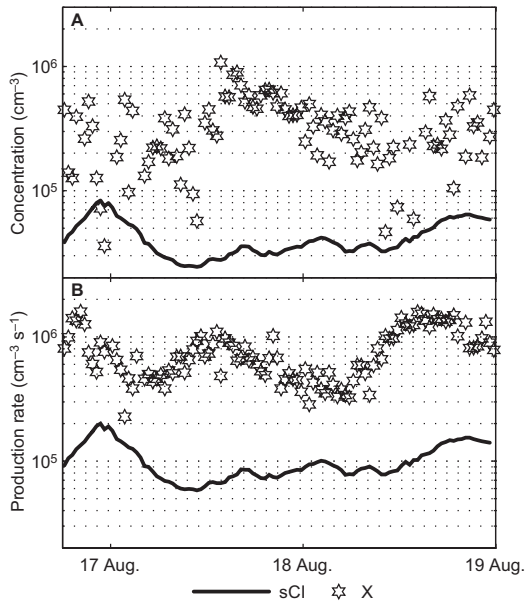

Fig. 8. Concentrations and production rates of all non-OH oxidants of SO_2 (X) and stabilized Criegee intermediates (sCIs) formed from the ozonolysis of monoterpenes. The X concentration and production rate were measured with the FR-CI-APi-TOF. The estimation of the sCI concentration and production rate was based on measured monoterpene and ozone concentrations. Only high quality X measurements are shown (*see* Fig. 4).

The X concentration showed weak negative correlations with the sCI concentration and production rate at the 95% confidence level (Table 1). The X production rate had positive correlations and the X lifetime negative correlations with the sCI concentration and production rate. This correlation analysis and Fig. 8 indicate that the sCI estimations followed the temporal patterns in the X measurements only partly, with the most pronounced disagreement between the X and sCI concentration. However, more measurements are needed to reveal the typical diurnal cycles of the X concentration and production rate at the measurement site.

Conclusions

The FR-CI-APi-TOF instrument showed promising potential for developing into a reliable field instrument. Approximately 60% of the first field measurements were successful in terms of the

linear relation between the H_2SO_4 concentration measured during the SO_2 injections and the X–SO_2 reaction time. However, the uncertainties in the determination of the X concentration and production rate were high, mainly due to the linear fits of Eq. 1 to only four observations. Adding more injectors to the flow reactor would probably decrease the uncertainties and consequently increase the proportion of high quality measurements. Laboratory experiments are still needed to better characterise the instrument response at different SO_2, ozone and alkene concentrations.

As demonstrated by the measurements during the second period, the X production rate had a diurnal cycle with a daytime maximum and a nighttime minimum. The temporal variation in the X concentration was less regular. The estimated concentration and production rate of sCIs from the ozonolysis of monoterpenes exhibited different temporal behaviour and were consistently lower than the X concentration and production rate. Also the ambient H_2SO_4 concentration was lower than the X concentration, which suggested that the oxidation of SO_2 was not the only important loss mechanism of X.

The correlations of the X concentration, production rate and apparent lifetime with monoterpene, ozone, SO_2 and H_2SO_4 concentrations did not reveal a consistent picture of the X chemistry at the measurement site. However, the number of measurements was very limited and longer observation periods with additional OH measurements are needed. In summary, the methods and measurements presented here offer a baseline for future instrument development and field measurements of X.

Acknowledgements: Arnaud P. Praplan is acknowledged for his help with the H_2SO_4 calibration, the tofTools team for providing tools for the mass spectrometry analysis and the staff of the SMEAR II station for their comprehensive assistance in all practicalities. This work was supported by the Academy of Finland (projects 1118615, 1139656 and 1251427), the Advanced Grant program of the European Research Council (project 227463) and the CRAICC project of the Nordic Top-level Research Initiative.

References

Beames J.M., Liu F., Lu L. & Lester M.I. 2012. Ultraviolet spectrum and photochemistry of the simplest Criegee intermediate CH_2OO. *J. Am. Chem. Soc.* 134: 20045–20048.

Beames J.M., Liu F., Lu L. & Lester M.I. 2013. UV spectroscopic characterization of an alkyl substituted Criegee intermediate CH_3CHOO. *J. Chem. Phys.* 138: 244307.

Benson D.R., Young L.-H., Rifkha Kameel F. & Lee S.-H. 2008. Laboratory-measured nucleation rates of sulfuric acid and water binary homogeneous nucleation from the SO_2 + OH reaction. *Geophys. Res. Lett.* 35: L11801, doi:10.1029/2008GL033387.

Berndt T., Jokinen T., Mauldin R.L.III, Petäjä T., Herrmann H., Junninen H., Paasonen P., Worsnop D.R. & Sipilä M. 2012. Gas-phase ozonolysis of selected olefins: the yield of stabilized Criegee intermediate and the reactivity toward SO_2. *J. Phys. Chem. Lett.* 3: 2892–2896.

Berresheim H., Elste T., Plass-Dülmer C., Eisele F.L. & Tanner D.J. 2000. Chemical ionization mass spectrometer for long-term measurements of atmospheric OH and H_2SO_4. *Int. J. Mass Spectrom.* 202: 91–109.

Berresheim H., Adam M., Monahan C., O'Dowd C., Plane J.M.C., Bohn B. & Rohrer F. 2014. Missing SO_2 oxidant in the coastal atmosphere? — Evidence from high resolution measurements of OH and atmospheric sulfur compounds. *Atmos. Chem. Phys. Discuss.* 14: 1159–1190.

Bonn B. & Moortgat G.K. 2003. Sesquiterpene ozonolysis: origin of atmospheric new particle formation from biogenic hydrocarbons. *Geophys. Res. Lett.* 30(11): 1585, doi:10.1029/2003gl017000.

Bork N., Kurtén T. & Vehkamäki H. 2013a. Exploring the atmospheric chemistry of $O_2SO_3^-$ and assessing the maximum turnover number of ion-catalysed H_2SO_4 formation. *Atmos. Chem. Phys.* 13: 3695–3703.

Bork N., Loukonen V. & Vehkamäki H. 2013b. Reactions and reaction rate of atmospheric SO_2 and $O_3^-(H_2O)_n$ collisions via molecular dynamics simulations. *J. Phys. Chem. A* 117: 3143–3148.

Boy M., Mogensen D., Smolander S., Zhou L., Nieminen T., Paasonen P., Plass-Dülmer C., Sipilä M., Petäjä T., Mauldin L., Berresheim H. & Kulmala M. 2013. Oxidation of SO_2 by stabilized Criegee intermediate (sCI) radicals as a crucial source for atmospheric sulfuric acid concentrations. *Atmos. Chem. Phys.* 13: 3865–3879.

Eisele F.L. & Tanner D.J. 1991. Ion-assisted tropospheric OH measurements. *J. Geophys. Res.* 96(D5): 9295–9308.

Eisele F.L. & Tanner D.J. 1993. Measurement of the gas phase concentration of H_2SO_4 and methane sulfonic acid and estimates of H_2SO_4 production and loss in the atmosphere. *J. Geophys. Res.* 98(D5): 9001–9010.

Hakola H., Tarvainen V., Bäck J., Ranta H., Bonn B., Rinne J. & Kulmala M. 2006. Seasonal variation of mono- and sesquiterpene emission rates of Scots pine. *Biogeosciences* 3: 93–101.

Hanson D.R. & Eisele F. 2000. Diffusion of H_2SO_4 in humidified nitrogen: hydrated H_2SO_4. *J. Phys. Chem. A* 104: 1715–1719.

Hari P. & Kulmala M. 2005. Station for Measuring Ecosystem–Atmosphere Relations (SMEAR II). *Boreal Env. Res.* 10: 315–322.

Harrison R.M., Yin J., Tilling R.M., Cai X., Seakins P.W., Hopkins J.R., Lansley D.L., Lewis A.C., Hunter M.C.,

Heard D.E., Carpenter L.J., Creasey D.J., Lee J.D., Pilling M.J., Carslaw N., Emmerson K.M., Redington A., Derwent R.G., Ryall D., Mills G. & Penkett S.A. 2006. Measurement and modelling of air pollution and atmospheric chemistry in the U.K. West Midlands conurbation: overview of the PUMA consortium project. *Sci. Total Environ.* 360: 5–25.

Heard D.E. & Pilling M.J. 2003. Measurement of OH and HO_2 in the troposphere. *Chem. Rev.* 103: 5163–5198.

Jiang L., Xu Y. & Ding A. 2010. Reaction of stabilized Criegee intermediates from ozonolysis of limonene with sulfur dioxide: ab initio and DFT study. *J. Phys. Chem. A* 114: 12452–12461.

Jokinen T., Sipilä M., Junninen H., Ehn M., Lönn G., Hakala J., Petäjä T., Mauldin R.L.III, Kulmala M. & Worsnop D.R. 2012. Atmospheric sulphuric acid and neutral cluster measurements using CI-APi-TOF. *Atmos. Chem. Phys.* 12: 4117–4125.

Junninen H., Lauri A., Keronen P., Aalto P., Hiltunen V., Hari P. & Kulmala M. 2009. Smart-SMEAR: on-line data exploration and visualization tool for SMEAR stations. *Boreal Env. Res.* 14: 447–457.

Junninen H., Ehn M., Petäjä T., Luosujärvi L., Kotiaho T., Kostiainen R., Rohner U., Gonin M., Fuhrer K., Kulmala M. & Worsnop D.R. 2010. A high-resolution mass spectrometer to measure atmospheric ion composition. *Atmos. Meas. Tech.* 3: 1039–1053.

Kjaergaard H.K., Kurtén T., Nielsen L.B., Jørgensen S. & Wennberg P.O. 2013. Criegee intermediates react with ozone. *J. Phys. Chem. Lett.* 4: 2525–2529.

Kulmala M., Kontkanen J., Junninen H., Lehtipalo K., Manninen H.E., Nieminen T., Petäjä T., Sipilä M., Schobesberger S., Rantala P., Franchin A., Jokinen T., Järvinen E., Äijälä M., Kangasluoma J., Hakala J., Aalto P.P., Paasonen P., Mikkilä J., Vanhanen J., Aalto J., Hakola H., Makkonen U., Ruuskanen T., Mauldin R.L.III, Duplissy J., Vehkamäki H., Bäck J., Kortelainen A., Riipinen I., Kurtén T., Johnston M.V., Smith J.N., Ehn M., Mentel T.F., Lehtinen K.E.J., Laaksonen A., Kerminen V.-M. & Worsnop D.R. 2013. Direct observations of atmospheric aerosol nucleation. *Science* 339: 943–946.

Kurtén T., Bonn B., Vehkamäki H. & Kulmala M. 2007. Computational study of the reaction between biogenic stabilized Criegee intermediates and sulfuric acid. *J Phys. Chem. A* 111: 3394–3401.

Kurtén T., Lane J.R., Jørgensen S. & Kjaergaard H.G. 2011. A computational study of the oxidation of SO_2 to SO_3 by gas-phase organic oxidants. *J. Phys. Chem. A* 115: 8669–8681.

Kürten A., Rondo L., Ehrhart S. & Curtius J. 2012. Calibration of a chemical ionization mass spectrometer for the measurement of gaseous sulfuric acid. *J. Phys. Chem. A* 116: 6375–6386.

Li J., Ying Q., Yi B. & Yang P. 2013. Role of stabilized Criegee Intermediates in the formation of atmospheric sulfate in eastern United States. *Atmos. Environ.* 79: 442–447.

Mauldin R.L.III, Frost G.J., Chen G., Tanner D.J., Prevot A.S.H., Davis D.D. & Eisele F.L. 1998. OH measurements during the First Aerosol Characterization Experiment (ACE 1): observations and model comparisons. *J. Geophys. Res.* 103(D13): 16713–16729.

Mauldin R.L.III, Tanner D.J., Heath J.A., Huebert B.J. & Eisele F.L. 1999. Observations of H_2SO_4 and MSA during PEM-Tropics-A. *J. Geophys. Res.* 104(D5): 5801–5816.

Mauldin R.L.III, Berndt T., Sipilä M., Paasonen P., Petäjä T., Kim S., Kurtén T., Stratmann F., Kerminen V.-M. & Kulmala M. 2012. A new atmospherically relevant oxidant of sulphur dioxide. *Nature* 488: 193–197.

Percival C.J., Welz O., Eskola A.J., Savee J.D., Osborn D.L., Topping D.O., Lowe D., Utembe S.R., Bacak A., McFiggans G., Cooke M.C., Xiao P., Archibald A.T., Jenkin M.E., Derwent R.G., Riipinen I., Mok D.W.K., Lee E.P.F., Dyke J.M., Taatjes C.A. & Shallcross D.E. 2013. Regional and global impacts of Criegee intermediates on atmospheric sulphuric acid concentrations and first steps of aerosol formation. *Faraday Discuss.* 165, 45, doi:10.1039/c3fd00048f.

Petäjä T., Mauldin R.L.III, Kosciuch E., McGrath J., Nieminen T., Paasonen P., Boy M., Adamov A., Kotiaho T. & Kulmala M. 2009. Sulfuric acid and OH concentrations in a boreal forest site. *Atmos. Chem. Phys.* 9: 7435–7448.

Pierce J.R., Evans M.J., Scott C.E., D'Andrea S.D., Farmer D.K., Swietlicki E. & Spracklen D.V. 2013. Weak global sensitivity of cloud condensation nuclei and the aerosol indirect effect to Criegee + SO_2 chemistry. *Atmos. Chem. Phys.* 13: 3163–3176.

Rinne J., Bäck J. & Hakola H. 2009. Biogenic volatile organic compound emissions from the Eurasian taiga: current knowledge and future directions. *Boreal Env. Res.* 14: 807–826.

Sander S.P. & Watson R.T. 1981. A kinetics study of the reaction of SO_2 with CH_3O_2. *Chem. Phys. Lett.* 77: 473–475.

Sarwar G., Fahey K., Kwok R., Gilliam R.C., Roselle S.J., Mathur R., Xue J., Yu J. & Carter W.P.L. 2013. Potential impacts of two SO_2 oxidation pathways on regional sulfate concentrations: aqueous-phase oxidation by NO_2 and gas-phase oxidation by stabilized Criegee intermediates. *Atmos. Environ.* 68: 186–197.

Sipilä M., Berndt T., Petäjä T., Brus D., Vanhanen J., Stratmann F., Patokoski J., Mauldin R.L.III, Hyvärinen A.-P., Lihavainen H. & Kulmala M. 2010. The role of sulfuric acid in atmospheric nucleation. *Science* 327: 1243–1246.

Stone D., Whalley L.K. & Heard D.E. 2012. Tropospheric OH and HO_2 radicals: field measurements and model comparisons. *Chem. Soc. Rev.* 41: 6348–6404.

Su Y.-T., Huang Y.-H., Witek H.A. & Lee Y.-P. 2013. Infrared absorption spectrum of the simplest Criegee intermediate CH_2OO. *Science* 340: 174–176.

Taatjes C.A., Shallcross D.E. & Percival C.J. 2014. Research frontiers in the chemistry of Criegee intermediates and tropospheric ozonolysis. *Phys. Chem. Chem. Phys.* 16: 1704–1718.

Taatjes C.A., Welz O., Eskola A.J., Savee J.D., Osborn D.L., Lee E.P.F., Dyke J.M., Mok D.W.K., Shallcross D.E. & Percival C.J. 2012. Direct measurement of Criegee intermediate (CH_2OO) reactions with acetone, acetaldehyde, and hexafluoroacetone. *Phys. Chem. Chem. Phys.* 14: 10391–10400.

Taatjes C.A., Welz O., Eskola A.J., Savee J.D., Scheer A.M., Shallcross D.E., Rotavera B., Lee E.P.F., Dyke J.M., Mok D.K.W., Osborn D.L. & Percival C.J. 2013. Direct measurements of conformer-dependent reactivity of the Criegee intermediate CH_3CHOO. *Science* 340: 177–180.

Taipale R., Ruuskanen T.M., Rinne J., Kajos M.K., Hakola H., Pohja T. & Kulmala M. 2008. Technical Note: Quantitative long-term measurements of VOC concentrations by PTR-MS — measurement, calibration, and volume mixing ratio calculation methods. *Atmos. Chem. Phys.* 8: 6681–6698.

Weber R.J., Marti J.J., McMurry P.H., Eisele F.L., Tanner D.J. & Jefferson A. 1996. Measured atmospheric new particle formation rates: implications for nucleation mechanisms. *Chem. Eng. Commun.* 151: 53–64.

Welz O., Savee J.D., Osborn D.L., Vasu S.S., Percival C.J., Shallcross D.E. & Taatjes C.A. 2012. Direct kinetic measurements of Criegee intermediate (CH_2OO) formed by reaction of CH_2I with O_2. *Science* 335: 204–207.

Vereecken L., Harder H. & Novelli A. 2012. The reaction of Criegee intermediates with NO, RO_2, and SO_2, and their fate in the atmosphere. *Phys. Chem. Chem. Phys.* 14: 14682–14695.

Vereecken L. 2013. Lifting the veil on an old mystery. *Science* 340: 154–155.

Witter M., Berndt T., Böge O., Stratmann F. & Heintzenberg J. 2002. Gas-phase ozonolysis: rate coefficients for a series of terpenes and rate coefficients and OH yields for 2-methyl-2-butene and 2,3-dimethyl-2-butene. *Int. J. Chem. Kinet.* 34: 394–403.

Zhang R. 2010. Getting to the critical nucleus of aerosol formation. *Science* 328: 1366–1367.